Energy dissipation capacity of shear link in rehabilitated reinforced concrete frame using eccentric steel bracing

G. Ghodrati Amiri[1] and A. Gholamrezatabar[2]

[1] *Professor, Center of Excellence for Fundamental Studies in Structural Engineering, College of Civil Engineering, Iran University of Science & Technology, P.O. Box 16765-163, Narmak,Tehran 16846, Iran*
[2] *Graduate Student, Faculty of Engineering, Shomal University, Amol, Iran*
E-mail: ghodrati@iust.ac.ir, ab_gholamrezatabar@yahoo.com

ABSTRACT :

Capacity of energy dissipation of shear link as a source of energy dissipation in reinforced concrete (RC) building rehabilitated using eccentric steel bracing is investigated. Some RC braced frames are analyzed subjected to strong ground motion. The focus of this study is mostly on the quantity of energy dissipated in shear link and its effectiveness on seismic performance. Height-wise distribution of steel bracing in the RC frame is changed to develop a better understanding of impact of shear link on seismic performance. Various values of KL/r are examined to investigate the link design parameters on its hysteric energy. The results show that shear link energy dissipation capacity can improve seismic performance of RC buildings.

KEYWORDS: Energy dissipation; Reinforced concrete; Retrofit; Eccentric steel brace; Shear link

1. INTRODUCTION

In the recent years various techniques were examined and investigated by different researchers to upgrade the seismic behaviors of existing buildings before subjected to futures earthquakes. One of popular and expected strategy for retrofitting of non-ductile or intermediate moment resisting frames is using concentric and eccentric steel bracing techniques. These methods provide different advantages simultaneously: (a) the ability to accommodate opening; (b) minimal added weight to the structures; (c) easy and fast installing and implementing. Eccentricity in bracing; however; is a smart method that engineers used to provide a segment to act as a fuse. The eccentrically braced frame (EBF) with vertical link contains a short segment that is connected to the chovern brace elements as a critical segment. This segment-called shear or flexural link- yields either in shear or in flexure. This system, which relies on the yielding of a link, has been proved that provide ductility and energy dissipation source under sever cyclic loading. In other words the EBF systems performances are directly related to the strength and ductility of links. Well-designed links provide a suitable source of energy dissipation. Different provisions prepare guideline for link designing. All of them try to define some limits to restrict rotations and slenderness of links. In this paper, the emphasis is upon the energy dissipation capacity of shear links in retrofitted RC frames using eccentric steel bracing elements. To expand the previous study, nonlinear dynamic analysis of a single story braced frames using various KL/r and t_f / t_w values were conducted to investigate the effect of these parameters on the hysteric energy.

2. RC BUILBIG AND RETROFIT SCHEM

As shown in Fig.1, three stories non-ductile RC frame with five spans was modeled. This building was designed for gravity load. Ghobarah and Aboue Elfath (2001) modeled selected building and studied seismic behavior of rehabilitated frame using various ground motions. The concrete strength is 21Mpa and steel yield strength is 350Mpa. The exterior columns are 300×300mm reinforced using 4-19mm diameter bares and interior columns are 400×400mm reinforced using 8-19mm diameter bars. Beams are 600×250mm for all three stories. Exterior beams are reinforced using 3-19mm diameter bars at the top and 2-19 mm diameter bars at the bottom. Interior beams are reinforced using 5-19mm diameter bars at the top and 2-19 mm diameter bars at the bottom. The thickness of slab is 50mm.

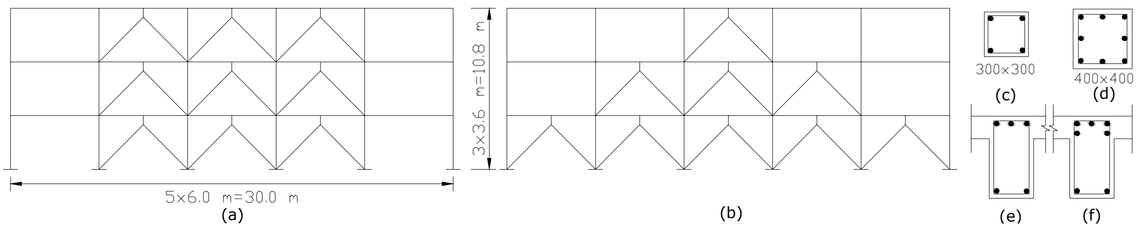

Figure 1 Retrofit cases for non-ductile three stories RC frame (a) First Case (FC) (b) Second Case (SC) (c) external columns (d) internal columns (e) external beams (f) internal beams

3. VERTICAL SHEAR LINK MODELING

Few researches attempted to develop link models for analytical modeling and dynamic inelastic analysis of EBF system. Ricles and Popov (1987) modeled shear-link elements as linear beam element with three nonlinear hinges at the end to represent shear force and a moment. Assuming a bilinear force-deformation relationship for each hinges, the combination in parallel at the end of the element result in a multi-linear relationship for the shear and the moment (Figs.2, 3). They define the governing parameters of the multi-linear shear force-deformation and bending moment-rotation relationships according to experimental tests on vertical shear links. Ramadan and Ghobarah (1995) modeled the link as a linear beam element with six nonlinear rotational and translational springs at each end. Rotational bilinear springs were represented by multi-linear function shown in Fig.2. Also translational bilinear spring represented by multi-linear function is shown in Fig.3. In this research vertical steel link represented by linear cantilever element with only two inelastic rotational and transitional springs at the fixed end. Each of the spring follow the moment-rotation and shear force-lateral displacement relationship. Dimensions of links were selected according to their plastic deformation capacity. Links were designed to remain in CP (Collapse Prevention) performance level while the frame pushed to target displacement during nonlinear analysis. The value of M_y and V_y are considered equal to M_p and $0.9V_p$ respectively. The other parameters are given as:

1. for shear (V value) and moment (M value)

$$V_{y1} = V_y \qquad M_{y1} = M_y$$
$$V_{y2} = 1.06V_y \qquad M_{y2} = 1.03M_y$$
$$V_{y3} = 1.12V_y \qquad M_{y3} = 1.06M_y$$

2. The value of the stiffness

$$K_{2V} = 0.03K_{1V} \qquad K_{2M} = 0.03K_{1M}$$
$$K_{3V} = 0.015K_{1V} \qquad K_{3M} = 0.015K_{1M}$$
$$K_{4V} = 0.002K_{1V} \qquad K_{4M} = 0.002K_{1M}$$

The value of K_{1M} and K_{1V} can be calculated as: $K_{1M} = 3EI/e$ $\qquad K_{1V} = GA_{web}/e$

Where E is elasticity modules, I is the moment of inertia of the link cross section, G is the modules of rigidity of steel and A_{web} is the area of the web of link section.

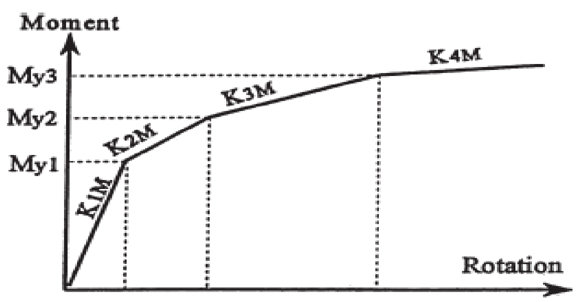

Figure 2 Moment-rotational relationship of a link (Ghobarah and Abou Elfath , 2001)

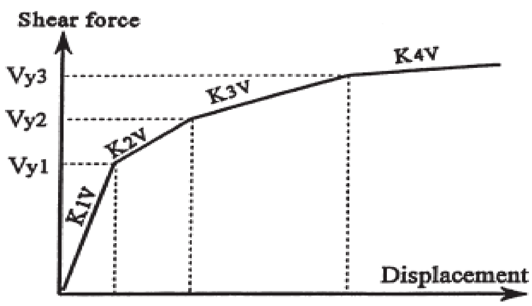

Figure 3 Shear force-deformation relationship of a link (Ghobarah and Abou Elfath , 2001)

4. NONLINEAR DYNAMIC ANALYSIS

Three ground motions were used in the nonlinear dynamic analyses (Table 1). The frames were subjected to listed recodes to investigate seismic behavior of rehabilitated frames. The seismic behaviors of retrofitted buildings were evaluated in term of input energy, hysteric energy and the ratio of them. $P-\delta$ effects were included in the analyses, and 5% damping was used.

Table 1 Selected ground motions

Record No.	Earthquake	Date	Site	PGA (g)	Duration (S)
1	Tabas	1978/09/16	Tabas, Iran	0.852	32.84
2	Imperial valley	1940/5/18	El Centro, USA	0.313	24.42
3	Naghan	1977/04/06	Naghan, Iran	0.720	5.0

Concrete frames with two different brace distribution patterns were evaluated under scaled accelerations of three strong ground motions. Values of input energy and hysteretic energy were calculated during excitation. Effect of brace distribution along the height of frames on input energy and hysteretic energy were investigated (Figs 4, 6, 8). As illustrated in Fig.4 input energy and hysteretic energy were almost zero during primary and weak motions. As the level of excitation suddenly increases, input energy valves increase considerably. Because links absorbed energy is related to nonlinear deformations so links hysteretic energy increase in different manner from input energy. Hysteretic energy gradually increases based on shear plastic deformation. Due to that shear links seismic behavior can be discriminate in three parts. First part observed during weak motion. In this primary period more than 50 percent to 90 percent of input energy dissipated by links nonlinear deformation. It means most of the input energy dissipated by links. This period is longer for Tabas and Naghan earthquakes and shorter for El Centro earthquake. Second part starts exactly after sudden fall in hysteretic and input energy ratio trend. In this critical period a sudden reduction observed in defined ratio. The reason can be interpreted according to earthquake acceleration. Strong motion after weak excitation promoted the input energy, while links hysteretic energy could not accommodate with it. As links hysteretic energy gradually increases the value of EH/EI increase to more than 60 percent. It is expected structural damages spread to beams and columns in second period. This period is shorter for Tabas earthquake (Fig.5) and longer for El Centro and Naghan (Figs7, 9). Third part starts exactly from the end of second part and continues to the end of motion. Defined period can be estimated by straight line with constant value. Third last long period shows maximum potential of links energy dissipation capacity. Links dissipate almost 70 percent of input energy. Change in brace distribution along the height of frames has no spatial effect on hysteretic energy process. Of course it is notable that second case (SC) of brace distribution decreases the input energy and did not change the hysteretic energy. Due to that the ratio of them will be grater and consequently seismic performance of second case (SC) will improve. The same result was concluded by Ghobarah and Elfath (2001).

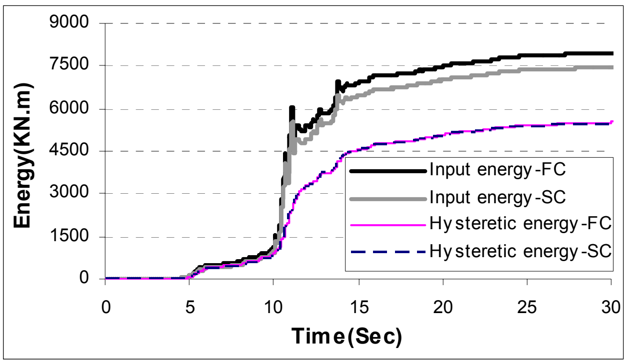

Figure 4 Input and hysteretic energies- Tabas

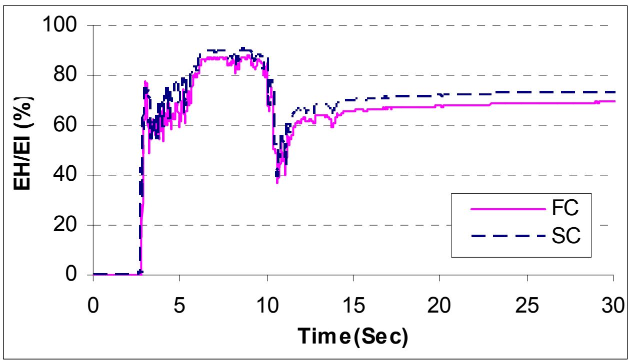

Figure 5 Input energy and hysteretic energy ratio- Tabas

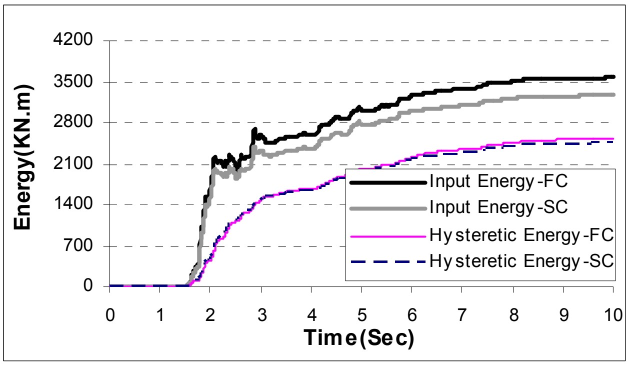

Figure 6 Input and hysteretic energies- El Centro

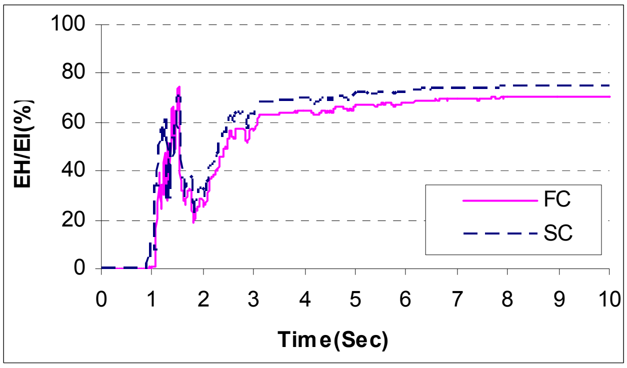

Figure 7 Input and hysteretic energy ratio- El Centro

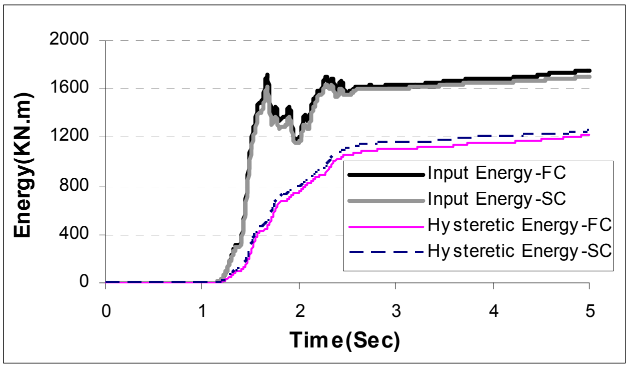

Figure 8 Input and hysteretic energies- Naghan

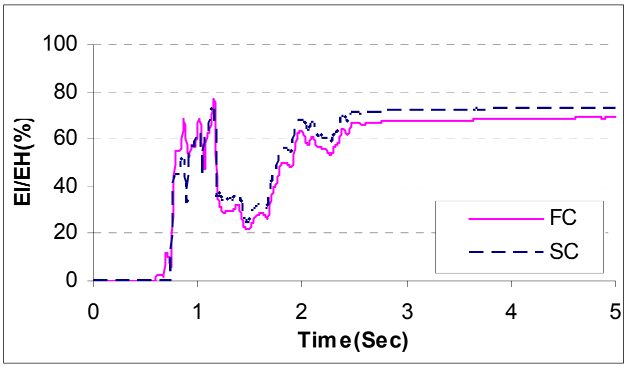

Figure 9 Input and hysteretic energy ratio- Naghan

5. PARAMETRIC STUDY

To expand the idea and follow the objective of this article a single degree of freedom RC frame with five bays is selected. Columns and beams were design to resist gravity dead and live loads. EBF bracing is provided by a single braced bay in mid span bay. Vertical shear link connected to the mid of the beam. As several researchers imply spatial consideration should be given to the connection between the vertical link and RC beam. The brace members provide negligible constraint to the link end against rotation in all cases. Links design to be sure that behave nonlinear during nonlinear analysis and remain in Collapse Prevention (CP) performance level when frames subjected to lateral load and pushed to target displacement. The purpose of this study is to evaluate effect of links design parameters on capacity of energy dissipation. Different seismic provisions prescribe procedure for eccentrically braced frames designing. All of them contain rules to restrict EBF inelastic action under strong ground motions. AISC seismic provisions conducted extensive experimental studies on Wide-Flange (WF) links of ASTM A36 steel and prepare a well established guidelines containing rules and limits for EBF with WF section links. Traditional and new limits of seismic provisions try to restrict the flange width-thickness ratio, $b_f / 2t_f$, according to experimental tests. A36 specified 8.5 for flange thickness ratio and A992 steel consider 7.2 for mentioned ratio. The same researches were conducted to find limits for the length of shear links. Based on experimental data the formula of $e_{crit} = 2b_f t_f / t_w$ can be used for calculating the length of cavalier link (e) to ensure that the link yields primarily in shear. Where b_f and t_f are the width and thickness of flange and t_w is the web thickness of a wide flange section link. Acceptance criteria for the length of the links are classified in AISC Seismic Provisions. Current code allows an inelastic rotation of 0.08 rad for $e \le 1.6M_P / V_P$ (shear link) and 0.02 rad for $e \ge 2.6M_P / V_P$ (flexural link). Corresponding ratio for intermediate length can be found by linear interpolation. Selected wide flange sections for this study are listed in Table 2.
Nine different wide flange sections in three groups (sections with the same height) were chosen for nonlinear analyses. Values of flange slenderness, critical length for primary shear yielding, used length for links and links

slenderness were calculated and listed in Table 2. Selected sections have flange slenderness between almost 4 to 10 values. In each group one section exceed the seismically compact limit for flanges thickness. One section almost meet the limit of 8.5 for flange slenderness and the last section in group satisfy the defined limit explicitly. Several nonlinear dynamic analyses using scaled acceleration (0.35g) of three earthquakes (Table 1) were conducted to investigate the effect of introduced parameters on input energy, hysteretic energy and the energy dissipation capacity of links.

5.1. Input Energy

The effects of link dimensions on input energy were investigated (Figs.10, 11, 12). By increasing the cross-section area of link maximum input energy to RC frame decreased. Because links with bigger sectional dimensions have higher shear stiffens (K_V) and shear plastic strength (V_P). So the lateral stiffness of frames increase and consequently the amount of maximum input energy reduced. Differences in initial input energy for different links are negligible. As the ground acceleration gets stronger the input energy trend for each RC frames continues in a separate manner. As links stiffness increases the input energy trend to RC frame become smoother and sudden raise and fall in input energy values are not observed.

Table 2 Selected wide flange sections

Section	$\frac{b_f}{2t_w}$	$e_{crit} = \frac{2b_f t_f}{t_w}$	$e = L$	$\frac{1.6M_P}{V_P}$	KL/r
W200x21	10.472	0.341	0.3	0.593	3.508
W200x52	8.095	0.651	0.6	1.017	6.742
W200x86	5.070	0.662	0.6	0.941	6.494
W250x49	9.182	0.601	0.6	0.972	5.644
W250x73	8.940	0.839	0.8	0.817	7.253
W250x131	5.199	0.851	0.8	0.420	6.956
W310x79	8.698	0.843	0.8	1.588	6.042
W310x179	6.175	1.004	1.0	1.455	7.215
W310x226	4.452	1.021	1.0	0.890	6.963

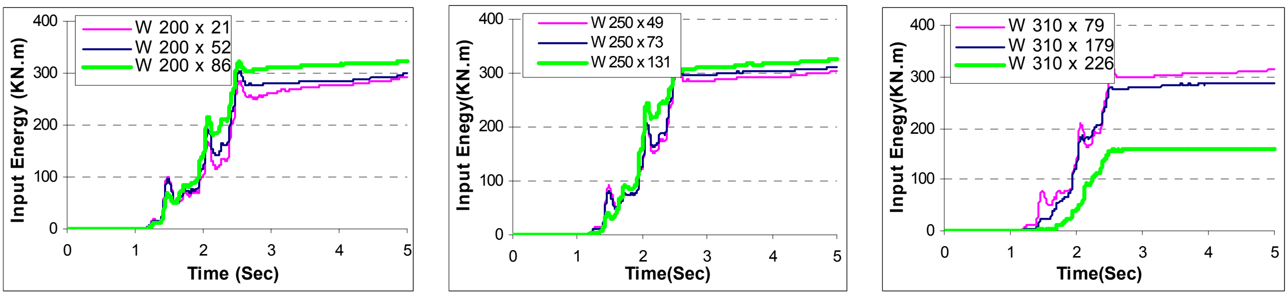

Figure 10 Input Energy - Naghan, PGA=0.35g, Damping=0.05

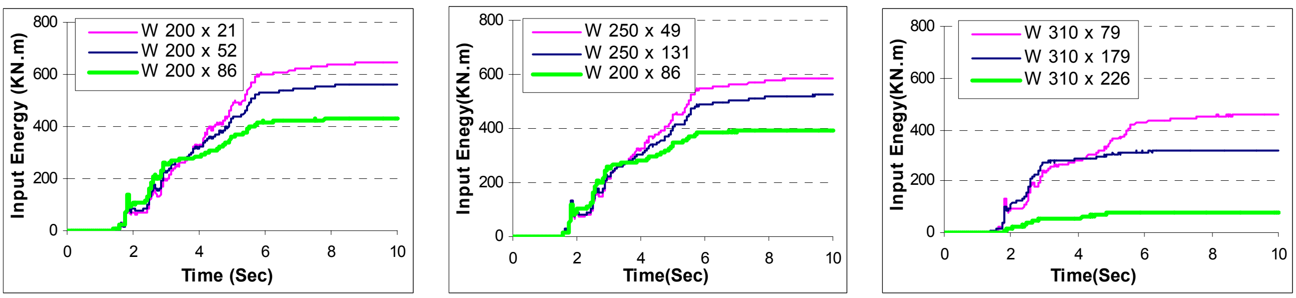

Figure 11 Input Energy - El Centro, PGA=0.35g, Damping=0.05

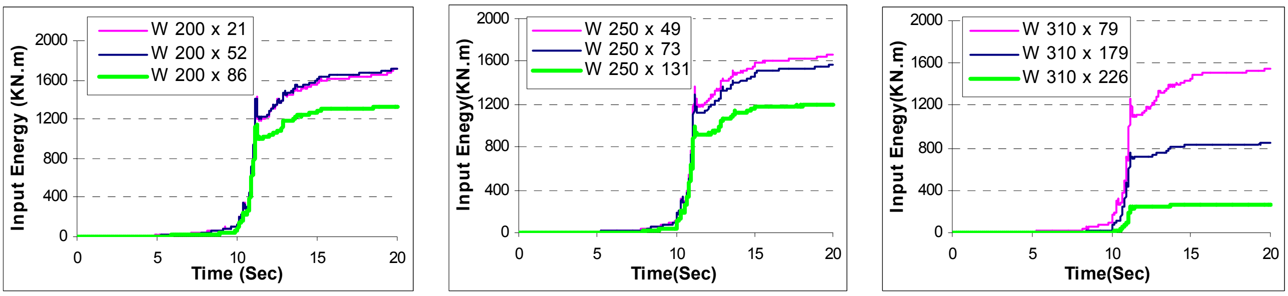

Figure 12 Input Energy - Tabas, PGA=0.35g, Damping=0.05

5.2. Hysteretic Energy

Figures 13, 14 and 15 represent the hysteretic energy of links due to nonlinear actions. In other words it states amount of absorbed energy during motions. Because link absorbed energy depends on nonlinear deformation capability and applied motions simultaneously, some interesting points occurred. During primary motions hysteretic energy was zero because link behaved elastically. As frame excited with strong motions, link became nonlinear and dissipated energy by nonlinear shear deformation. Third links in each group have higher hysteretic energy because have higher deformation capability. Of course W310x226 did not follow the rule, because link with W310x226 was not flexible enough to deform. Less nonlinear deformation caused less absorbed energy.

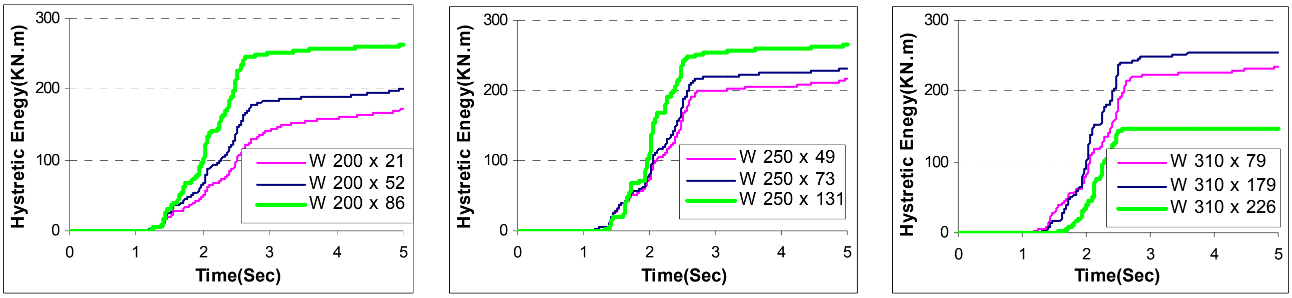

Figure 13 Hysteretic Energy - Naghan, PGA=0.35g, Damping=0.05

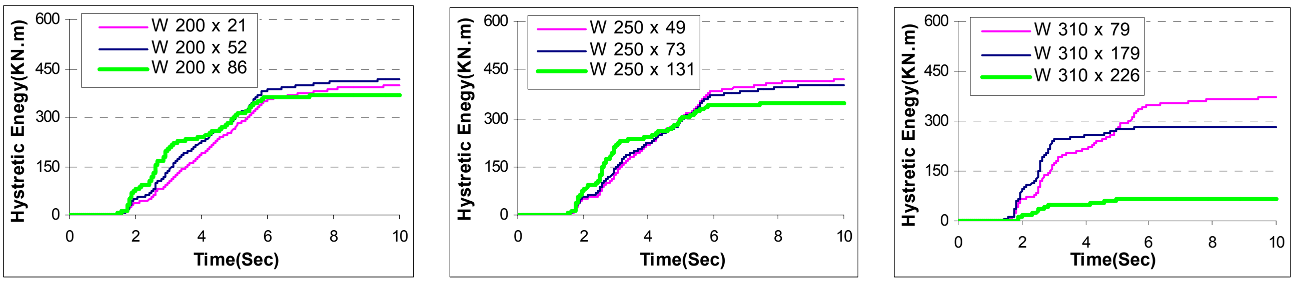

Figure 14 Hysteretic Energy - El Centro, PGA=0.35g, Damping=0.05

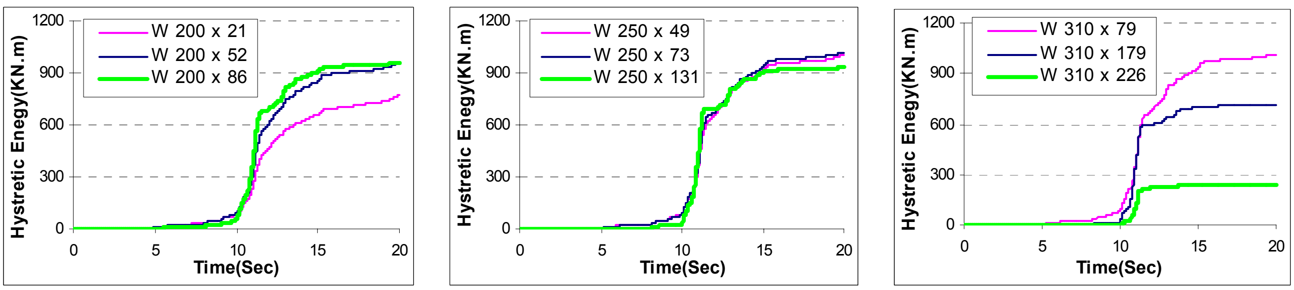

Figure 15 Hysteretic Energy - Tabas, PGA=0.35g, Damping=0.05

An interesting phenomenon occurred in linear part of hysteretic energy with constant value. As shown in Figs.14, 15 sometime maximum hysteretic energy of link with smaller section become higher than the maximum hysteretic energy of link with bigger section. This phenomenon can be attributed to the flexibility of links. By paying more consideration to the link stiffness we come to conclusion that although stiff link have higher hysteretic energy during strong excitations but flexible links absorb more input energy during last week motion and finally the cumulative hysteretic energy of flexible link promote more in compare with stiff links.

5.3. Hysteretic Energy and Input Energy Ratio

Hysteretic energy and input energy ratio show the capability of energy dissipation in structural elements. Table 3 summarized the results of nonlinear analyses for EBF RC frames. The ratio of these two types of meaningful energy used to estimate the level of structural damages during ground motions. Defined ratio shows the capacity of energy dissipation and absorbed damages by links. Also this ratio is correspondence to damage index. The seismic performance of retrofitted RC frames is investigated in term of hysteretic energy and input energy ratio. The seismic performance of rehabilitated fames is related to amount of input energy which is dissipated in the links that directly depends on energy dissipation capacity of links. According to the obtained values for the ratio, it seems more preferable to divided hysteretic energy and input energy ratio in to three regions. First region specified to the part of ratio that is almost zero. This region last longer or shorter based on link flexibility and earthquake acceleration intensity (Figs.16, 17, 18). This primary part is shorter for flexible links and longer for stiff links (Fig.18).

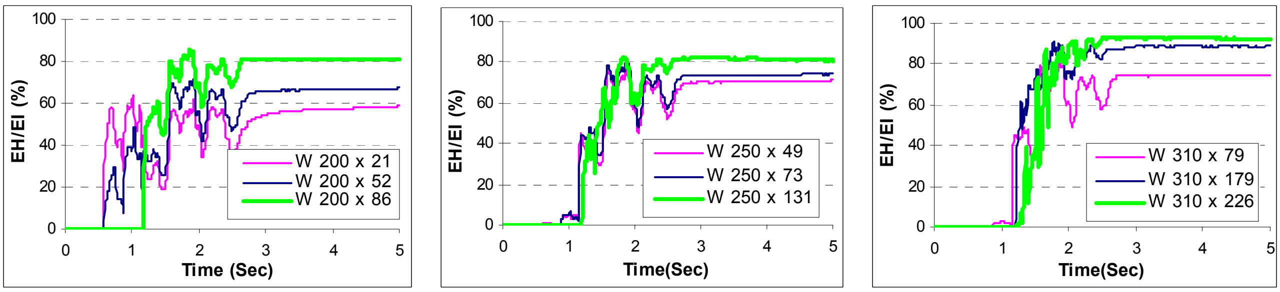

Figure 16 Input Energy and Hysteretic Energy Ratio- Naghan, PGA=0.35g, Damping=0.05

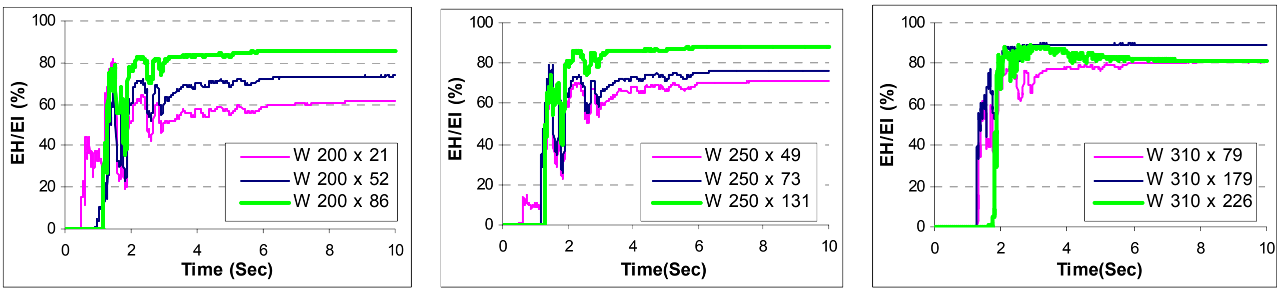

Figure 17 Input Energy and Hysteretic Energy Ratio- El Centro, PGA=0.35g, Damping=0.05

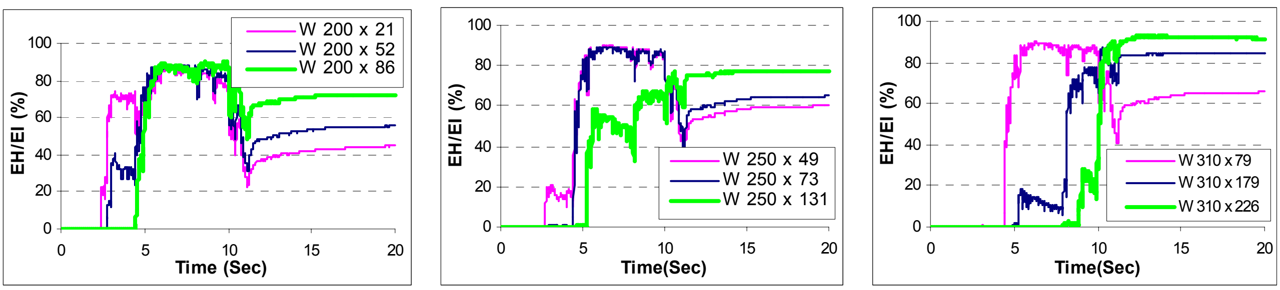

Figure 18 Input Energy and Hysteretic Energy Ratio- Tabas, PGA=0.35g, Damping=0.05

Table 3 Capacity of energy dissipation and plastic rotation of links with different sections under earthquakes

Section	Capacity of energy dissipation (%)			Rotation(γ)		
	Tabas	EL Centro	Naghan	Tabas	EL Centro	Naghan
W200x21	47	60	60	0.0833	0.0318	0.0331
W200x52	57	73	70	0.0279	0.0156	0.0150
W200x86	72	86	80	0.0304	0.0123	0.0116
W250x49	60	73	70	0.0375	0.0157	0.0142
W250x73	64	78	74	0.0262	0.0115	0.0099
W250x131	80	88	82	0.0181	0.0096	0.0087
W310x79	60	81	74	0.0258	0.0113	0.0098
W310x179	83	89	90	0.0104	0.0062	0.0048
W310x226	90	89	92	0.0048	0.0012	0.0029

Consequently structural damages in beams or columns are expected in RC frames retrofitted using stiff link in first primary motions because they behave nonlinear with time delay. Second region starts exactly after the end of first region or from the start of strong motions. In this region links undergo severe cyclic loading. It is essential to link behave nonlinear to absorb energy. As consequence of suddenly and repeatedly raise and fall in input energy under the applied motion, the hysteretic energy and input energy ratio vary between minimum (20%) and maximum (90%) values repeatedly. It states in second region damages may spread to beams and columns when input energy suddenly increase. Third region specified to the part of defined ratio trend that can be estimated or normalized with straight line. This line with constant value shows the capacity of energy dissipation for each link.

6. CONCLUTION

Current research estimates the capacity of energy dissipation of shear links up to almost 90 percent clearly under the effect of link design parameters and applied ground motions. Fortunately by respecting to the shear link length limits and flange slenderness none of them exceed the seismically limit of 0.08 rad for rotation. Links with second section in each group which have flange slenderness near to limit (8.5) seem to act the best.

REFERENCES

American Institute of Steel Construction, Inc. (AISC). (2005). Seismic provisions for structural steel buildings, Standard ANSI/AISC 341-05. Chicago (IL, USA).

Bush, T.D., Jones, E.A and Jirsa, J.O. (1991). Behavior of RC frame strengthened using structural-steel bracing. *Journal of Structural Engineering ASCE* **117:4**, 1115–1126.

Ghobarah, A., Abou Elfath, H.T. (2001). Rehabilitation of a reinforced concrete frame using eccentric steel bracing. *Journal of Structural Engineering, ASCE* **23:7**, 745-755.

Perera, P., Gomez, S. and Alarcon, E. (2004). Experimental and analytical study of Masonry infill reinforced frames retrofitted with steel braces. *Journal of Structural Engineering, ASCE* **130:12**, 2032-2039.

Ramadan, T., Ghobarah, A. (1995). Analytical model for shear–link behavior. *Journal of Structural Engineering, ASCE* **121:11**, 1574–1580.

Ricles, J.M., Popov, E.P. (1987). Dynamic analysis of seismically resistant eccentrically braced frames. Report No. UCB/EERC-86/07, Earthquake Engineering Research Center, University of California, Berkeley, California.

Taichiro, O., Michael, D.E. (2007). Cyclic loading behavior of EBF links constructed of ASTM A992 steel. *Journal of constructional steel research* **63:6**, 751-76.